ELSEVIER

International Journal of Mass Spectrometry 223–224 (2003) 355–363

International Journal of Mass Spectrometry

www.elsevier.com/locate/ijms

The relationship between covariance and anti-covariance mapping

D.A. Card[a,b], E.S. Wisniewski[b], D.E. Folmer[b,1], A.W. Castleman Jr[b,c,*]

[a] *Department of Chemistry, Photonics Research Center, United States Military Academy, West Point, NY 10996, USA*
[b] *152 Davey Laboratory, Department of Chemistry, The Pennsylvania State University, University Park, PA 16802, USA*
[c] *Department of Physics, The Pennsylvania State University, University Park, PA 16802, USA*

Received 11 November 2001; accepted 24 May 2002

Abstract

Pyridine clusters are subjected to intense femtosecond laser pulses at fluences around 10^{15} W cm^{-2} at 620 nm, which results in multiple ionization and concomitant Coulomb explosion. A combined covariance map is considered which can be viewed as the overlay of two maps that describe the statistical interaction of the resulting time-of-flight spectra of the pyridine clusters which lead to species having large values of kinetic energy. The combined map is constructed from ones involving both positive covariance values and anti-covariance values obtained in the same experimental study. Significantly, the individual points representing positive and anti-covariance effects arising from the ionization of the clusters via femtosecond laser pulses are found to be mutually exclusive of each other as exemplified in this pyridine study. Our extension of covariance mapping, which was originally formulated by Frasinski et al. for simple molecular interactions, and is further developed in the present study, elucidates the presence of competitive reactions within cluster systems by comparison of the two maps. (Int J Mass Spectrom 223–224 (2003) 355–363)

Keywords: Covariance mapping; Clusters; Femtosecond laser; Pyridine clusters; Coulomb explosion; Time-of-flight mass spectrometer

1. Introduction

The study of cluster ionization and dissociation is typically made by subjecting the system to changes of a single variable, thereafter observing a result. This sequence of events can lead to a depth of understanding about how a given parameter affects a system with quantitative measurements usually made through carefully measured averages. Averaging the results offers the ability to minimize the background noise while amplifying the signal. For example in time-of-flight mass spectrometry, the time-of-flight mass spectrum is commonly averaged for 500 or more times. Applying this technique and changing a single variable, correlations can be inferred between the system and the perturbed variable. While averaging the results improves the signal-to-noise ratio, the subtle interactions between ions can become lost.

Covariance mapping, pioneered by Frasinski et al. in a prolific series of papers, statistically bridged the chasm between the approach of averaging as opposed to the tedious coincidence method which typically involves working at the level of small events [1–10]. Previously, studies in multidimensional interactions

* Corresponding author. E-mail: awc@psu.edu
[1] Present address: The Food and Drug Administration, Washington, DC, USA.

1387-3806/02/$ – see front matter
PII S1387-3806(02)00928-4

required the system's parameters to be modified in order to establish this interaction relationship. Frasinski's findings suggested that only the original system was necessary to establish an interaction if a correlation of subtle signal oscillations was made [1]. These deviations, caused by the system parameters (e.g., in the case of clusters, the pulse nozzle, laser pulse power, electric field, etc.), carry with them the information connecting particles [1,11]. Frasinski argued that this information was especially key to determining whether a reaction was symmetric or asymmetric [2–4,6–10].

Frasinski et al., demonstrated the covariance approach involving small molecular species such as N_2, N_2O, and CO [1–10]. In their approach, they established the relationship between forward- and

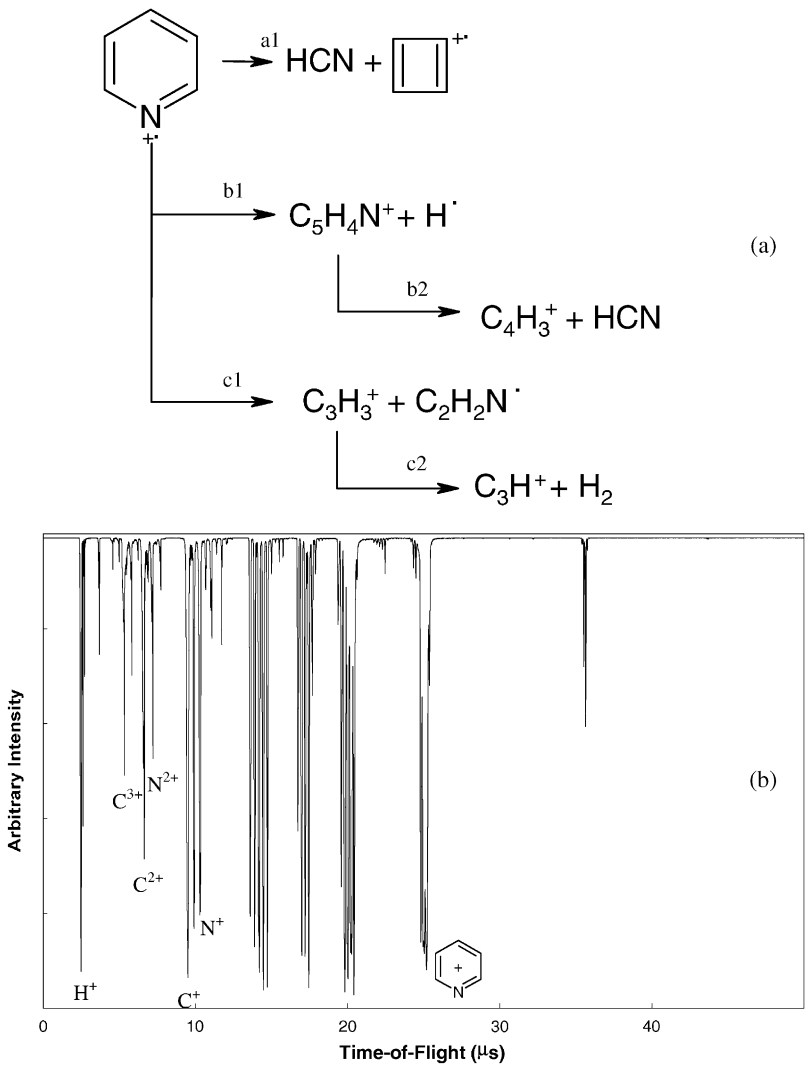

Fig. 1. The fragmentation of pyridine. (a) These fragmentation channels for pyridine were proposed based upon results of electron impact and collision induced ionization studies [16]. Reference [16] states these mechanisms lead to percent abundances in a1, b1, b2, and c1 of 70, 13, 36, and 13%, respectively. (b) Pyridine clusters strongly absorb femtosecond pulses at 620 nm and Coulomb explode primarily into multiply charged atoms. This is the average spectrum for 10,000 laser shots and is the byproduct of the covariance analysis.

backward-ejected fragments from a Coulomb explosion event. They reported only a single surface, which they appropriately named a "covariance map". Applying the covariance approach to clusters, we have found the presence of two surfaces. In cluster systems, several moieties may be present at once, and the interaction of a pulsed laser beam with these clusters can lead to a plethora of fragments—far more than with single molecules [11,12]. Moreover, studies elucidating Coulomb explosion continually suggested a fluence threshold whereby high fluences promoted Coulomb explosion and low fluences permitted only simple ionization [11,13]. When we pursued the approach of Frasinski et al., we found the presence of two surfaces describing the ionization regions defined by high and low fluences stated previously [11]. Other studies suggested this phenomenon was not unique, but defined at least two different ionization pathways or competitive mechanisms [11–14].

Coulomb explosion presents a perfect response to explore with covariance mapping. When a cluster encounters a high fluence (i.e., $>10^{15}\,\mathrm{W\,cm^{-2}}$) ultrafast laser pulse, multiple electrons are stripped and the cluster is left with a concomitant large charge. The repulsive presence of multiple charges in relative close proximity destabilizes the cluster and in some cases leads to fission of the cluster while in others directly to Coulomb explosion.

Three characteristic fragments (i.e., forward-ejected, backward-ejected, and ion-core) are formed in an explosion, which are defined in accordance with their travel towards a microchannel plate (MCP) detector [14]. In our experimental arrangement [11], the forward-ejected fragments are expelled directly toward a reflecting electric field (reflectron) where they are reflected toward the MCP and are detected unless their kinetic energy exceeds the reflecting potential of the reflectron. In the latter case, they maintain a forward trajectory and pass through the reflectron. Backward-ejected fragments are directed away from the MCP and if their kinetic energy is less than the repeller potential, they are turned around and follow their forward-ejected siblings, but with a slight time difference. Ion-core fragments move toward the MCP without energy from a Coulomb explosion; ion-core fragments can arise as the product of a single electron loss or due to ions born at the center of the cluster explosion where repelling forces of neighbors effectively cancel each other [14].

Pyridine is an aromatic heterocyclic compound with a single nitrogen atom. It is planar in the ground state and when ionized loses its first electron from the nitrogen atom [15]. Pyridine has been studied previously through electron impact and collision induced dissociation, [15–19] and more recently with ultrafast lasers [14,20]. Fig. 1 identifies the proposed mechanism for pyridine including both the ionization and dissociation processes.

2. Experimental

The experimental apparatus consists of a femtosecond laser, a cluster source and a time-of-flight mass spectrometer affixed with a reflectron. The femtosecond pulse generation system has been described in detail elsewhere [21]. Briefly, a femtosecond pulse is created when a continuous-wave argon ion laser focused into an Rhodamine 590 dye in a colliding pulse mode-locked arrangement. The beam is mode-locked with DODCI dye mixed in ethylene glycol. Amplification is achieved with Sulforhodamine 640 dye solution (50/50 methanol/water) irradiated with the second harmonic of a Nd:YAG laser. Prism pairs are used to recompress the pulse. An amplified beam of roughly 1 mJ per pulse with a fluence nearly $10^{15}\,\mathrm{W\,cm^{-2}}$ at the focal point is typically acquired.

Clusters are introduced by heating pyridine and entraining the vapor with helium gas. The mixture is then pulsed through a jet nozzle with a backing pressure of 2200 Torr into a vacuum chamber maintained near 1×10^{-6} Torr.

The mass spectrometer parallels the Wiley–McLaren design [22] coupled to a reflecting electric field (reflectron) [23]. Clusters are ionized with a femtosecond laser in between two charged plates on the time-of-flight axis and are thereafter accelerated by a field gradient. The ions encounter the reflectron after

traversing a 1.4 m field-free region and are repulsed through a 0.7 m field-free region toward an MCP.

3. Results and discussion

The primary objective of this paper is to show that the surfaces of covariance and anti-covariance maps are mutually exclusive. Although they originate from excitation of the same molecular system under identical conditions, the values obtained through the covariance analysis are dependent upon the fluctuation within the system, and as will be shown, these can be positive or negative. Moreover, a direct result of this analysis (see [11]) is that the presence of a covariance and anti-covariance surface establishes that both concomitant and competitive reactions are operative within the system.

When clusters are irradiated at high intensities, they are ejected over a broad distribution of angles away from the point of formation. Cluster ions, which are refocused following backward ejection, proceed toward the detector along with ones that are initially ejected in a forward direction. As described above, others with a single charge, born in the center of a Coulomb exploded cluster or simply ionized without Coulomb explosion, travel towards the MCP without additional kinetic energy. The backward- and forward-ejected ions may or may not be products of the same cluster ion. Thus, their intensities may differ depending on their birth. However, as described by Frasinski et al., the backward- and forward-ejected congeners would be coupled by equal covariances [1–10].

The parameters of the mass spectrometer, the kinetic energy imparted to an ion during Coulomb explosion, and the mass of the ion define its time-of-flight. Depending on the choice of the parameters, backward-ejected ions can overtake the ion-core [14]. Hence, the flight times of the respective ions need to be ascertained to ensure correct identification. In the present study, the forward-ejected, ion-core, and backward-ejected carbon cations arrive at approximately 9.898, 9.919, and 9.934 μs, respectively. These arrival times are based upon the carbon arrival time at 9.918 μs in the absence of Coulomb explosion.

During the course of our studies, a threshold was commonly found whereby one type of ion is preferentially produced over another. In an ammonia study, the intensities of the singly charged clusters were found to vary inversely with the intensities of Coulomb exploded fragments [11]. In a titanium–carbon study, interplay for the same progenitor led to parallel processes reported previously [12]. These processes are competitive and suggest a dependence on the laser fluence.

Normally cluster studies utilizing TOF mass spectrometry take advantage of the fact that various processes produce an *average intensity* value, which can be analyzed and interpreted. However, deviations in the ion intensity do occur because of slight fluctuations in the laser pulse or pulsed nozzle, and advantage is taken of these fluctuations in implementing the technique of covariance mapping.

Covariance mapping compares the changes in one measurement with another measurement, by way of a shot-by-shot analysis. Covariance is defined as the deviation in two measurements of two different species, just as the variance is the deviation in two measurements of the same species. Thus, the covariance analysis provides a measure of the linkage between two different variables, namely two different ions in the present case.

Mathematically, the covariance, $C(x, y)$ can be expressed by: [1,24,25]

$$C(x, y) = \langle (X - \langle X \rangle)(Y - \langle Y \rangle) \rangle$$

$$C(x, y) = \langle XY \rangle - \langle X \rangle \langle Y \rangle$$

$$C(x, y) = \frac{1}{N} \sum_{i=1}^{N} X_i(x) \cdot Y_i(y) - \left[\frac{1}{N} \sum_{i=1}^{N} X_i(x) \right] \left[\frac{1}{N} \sum_{i=1}^{N} Y_i(y) \right]$$

where $X_i(x)$ and $Y_i(y)$ represent ion intensities at some time-of-flight "x" or "y" for a particular ionization event "i". $C(x, y)$ is termed the covariance [24,25].

Positive values are plotted on a "covariance map" and negative values encompass the "anti-covariance map". Since $X_i(x)$ and $Y_i(y)$ are the same functions when x equals y, the value of $C(x, x)$ is the variance or the square of the standard deviation of the intensity—a positive quantity. The variance provides a degree of symmetry along the x–y axis of all covariance plots. Similarly, the mean function or the average time-of-flight (e.g., Fig. 1a) is defined as:

$$\bar{X}(x) = \frac{1}{N}\sum_{i=1}^{N} X_i(x)$$

In terms of a chemical reaction, two peaks are obviously coupled if both increase or decrease with each other. On the other hand, two peaks are anti-correlated if one increases while the other decreases. And if a peak remains unchanged when the other either increases or decreases they are, of course, uncorrelated. With three potential fragments for each ion resulting from an ionization event, the interaction displayed on covariance maps increases complexity. Consider the interactions of carbon in Fig. 2. While the diagonal members reduce to the variance, three off diagonal members or covariances occur when an ion-core is present. Nonetheless, similar representations are found as described by Frasinski's model. A representative covariance map for the pyridine system is shown in Fig. 3. The covariance indicates the coupling of the processes responsible for the formation of the respective species.

Next, we consider anti-covariance which represents competitive processes in the formation of the various ions identified in the plot. Fig. 4 is an overlaid map showing both covariances and anti-covariances for the pyridine system. The covariance data from Fig. 3 has been altered in color to appear only in blue, while anti-covariance data for this system is indicated by red data points. These maps were developed from an entire spectrum and enlarged to focus on the region between mass-to-charge ratios 1–12. Comparison of the two maps readily reveals that the points on the maps are mutually exclusive. Most importantly, though, note the red points of the anti-covariance map fall in the voids of the covariance map. Consider first the carbon-carbon interactions shown in detail in the insert at the upper right-hand corner of the figure. The points on the covariance map are defined

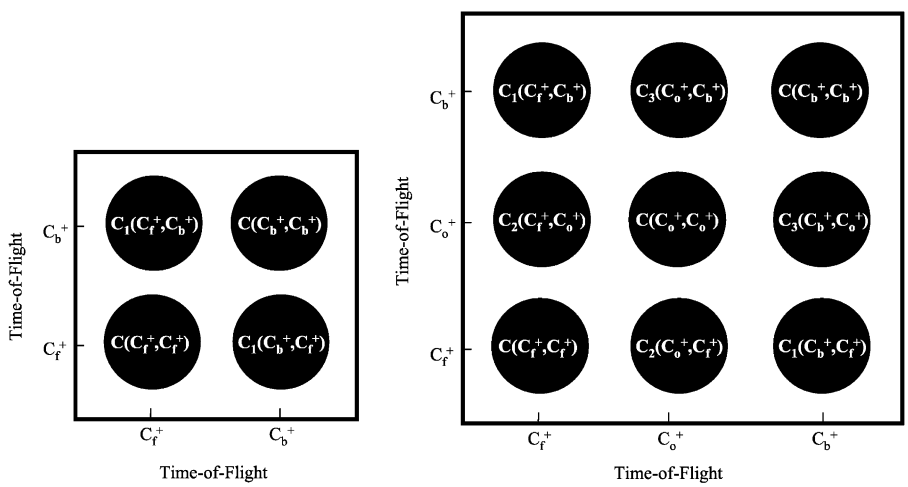

Fig. 2. Covariance interaction of the carbon cation. (a) Covariance pairs defined by Frasinski's method. The subscripts b and f denote backward and forward ejected peaks, respectively. (b) Covariance pairs can be defined for each coupling of the forward-ejected carbon, ion-core carbon, and backward-ejected carbon. Covariances of identical coupled pairs are equivalent and are denoted with subscripts. For example: $C_1(C_f{}^+, C_b{}^+) = C_1(C_b{}^+, C_f{}^+)$.

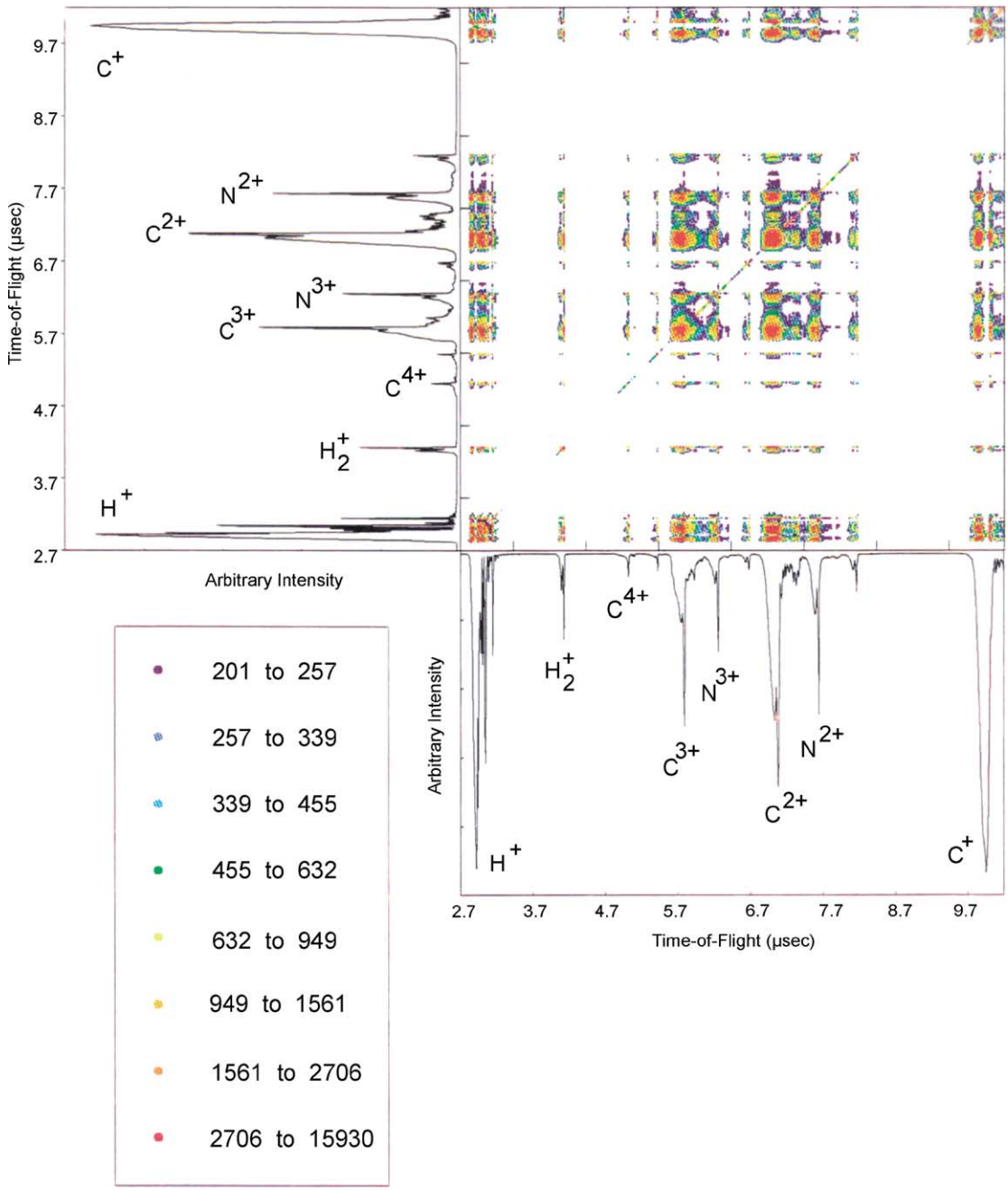

Fig. 3. Covariance map extracts for the pyridine system at mass-to-charge ratio 1–12. The extent of the correlation between various species is denoted by the color code.

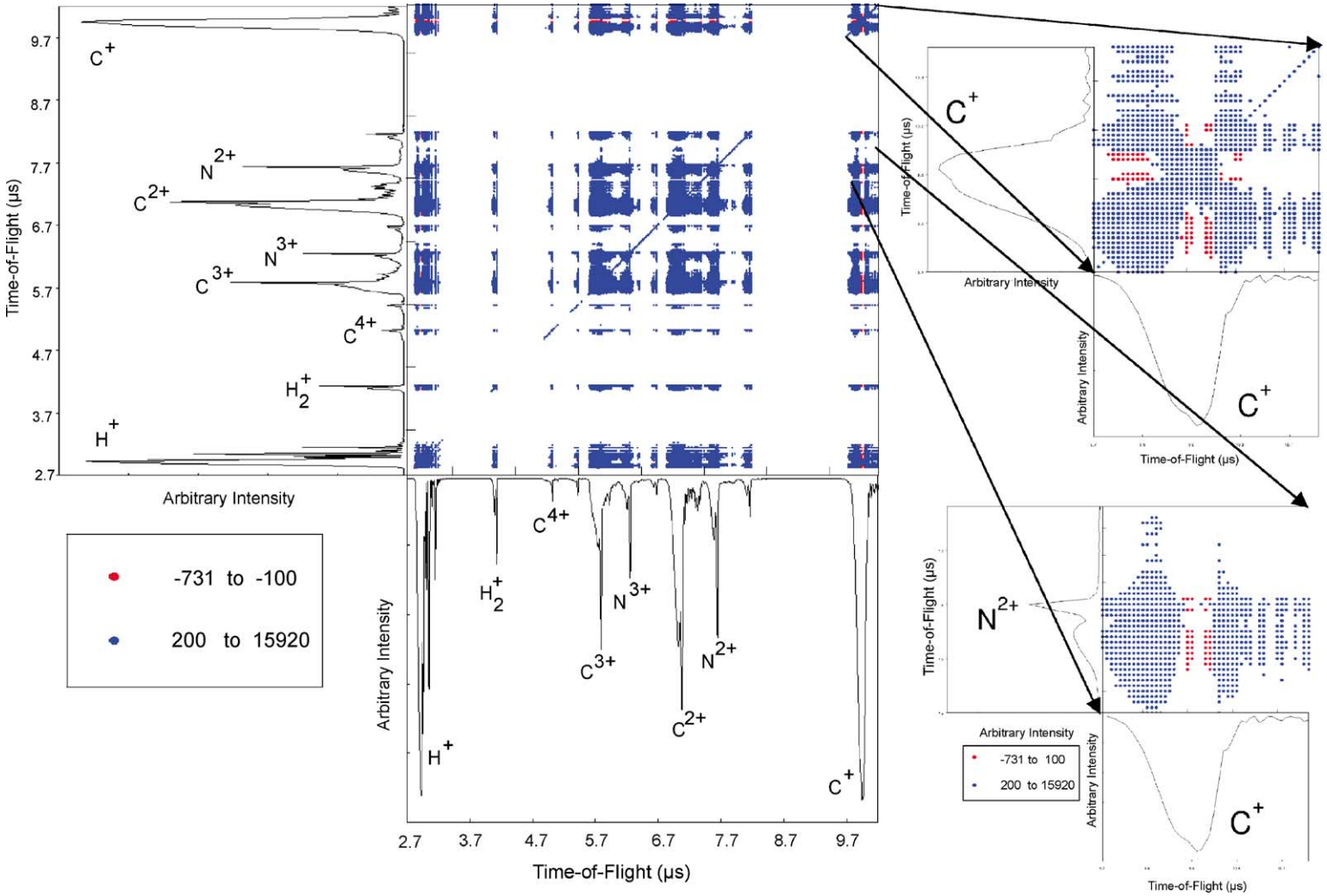

Fig. 4. Combined covariance and anti-covariance map extracts of pyridine. A covariance map and anti-covariance map were developed for pyridine; they are overlaid to emphasize that all points are mutually exclusive. This extract of the covariance map represents the possible interactions between ions having masses from the proton through the carbon cation. The 242,530 covariance values plotted in the original map were between 500 and 15,930. The 18,112 points in the original anti-covariance map represented all of the values between −100 and −1385. The abscissa and ordinate are the mean time-of-flight spectra and were calculated from the same data that was used to develop this covariance map.

by: (1) the variance of the three fragment interactions (forward-ejected, backward-ejected and zero kinetic energy ions) and (2) the covariance of the forward- and backward-ejected ions (e.g., C_1 from Fig. 2b). However, the carbon ions representing those born at the center of the cluster and hence having zero kinetic energy are anti-correlated with the forward- and backward-ejected carbons as defined by the anti-covariance data plotted in red.

A similar analysis is seen for interactions between C^+ and N^{2+}. Here, C^+ with zero kinetic energy release is clearly anti-correlated with the forward- and backward-ejected N^{2+}, indicating formation via competitive rather than concerted processes. Competition can best be visualized when considering parallel or consecutive reactions. For instance in Fig. 1a, if a single ionization event proceeds through pathway a1, then pathways b1 and c1 are momentarily inoperative. However, if we consider an ensemble, a1, b1, and c1 can occur simultaneously. Subtle fluctuations can promote one pathway and the ions produced vary. The pathway promoted would produce more product and the other pathway would result in less product, on average. These deviations define anti-covariance. However, if two products result from a Coulomb explosion, they would simultaneously increase and yield a positive covariance.

One of the goals of chemical dynamics is to effect the formation of chosen reaction products by influencing the course of a reaction. Pulse shaping is a technique that has been gaining considerable interest in this area of controlling the course of a chemical reaction [26–29]. The use of pulse shaping often uses genetic feedback algorithms to modify wavelength and intensity profiles of large bandwidth femtosecond laser pulses to maximize the generation of a particular reaction product. Covariance studies also can be utilized to not only correlate slight fluctuations between individual laser shots but also to correlate slight differences in pressure fluctuations, cluster distribution and laser pulse width and energy to determine varying conditions that may lead to preferred reaction products. While not a trivial problem, tagging each individual mass spectrum recorded in a covariance experiment with additional information regarding experimental conditions such as expansion pressure (with associated temperature), laser energy and laser pulse width would expand the enormous bank of knowledge currently yielded by covariance analysis.

4. Conclusion

Irradiation of clusters with high fluence, ultrafast lasers strips several electrons and causes repulsion between positively charged components within the cluster. When the ionized cluster undergoes Coulomb explosion, the net movement of all ions is toward the MCP because of a potential gradient in the ionization region. Ions thrust towards the MCP are forward-ejected ions; similarly ions directed away from the MCP initially and turned around by the potential gradient are backward-ejected ions. Ion-core fragments result either from a birth at the center of a Coulomb exploded cluster or from simple ionization.

The interaction of these fragments not only creates covariance from forward- and backward-ejected ions, as suggested by Frasinski et al., but also covariance pairs with the ion-core. These distinct covariance values are possibly based upon the foregoing analysis. These covariance can be positive and negative for the same ion depending upon their fragmentation pathway.

Acknowledgements

Financial support by the Air Force Office of Scientific Research, Grant Nos. F49620-94-1-0162 and F49620-01-1-0380., is gratefully acknowledged. Moreover, D. A. Card wishes to thank the Faculty Research and Development Fund from the Dean, United States Military Academy for travel funds.

References

[1] L.J. Frasinski, K. Codling, P.A. Hatherly, Science 246 (1989) 1029.
[2] L.J. Frasinski, K. Codling, P.A. Hatherly, Phys. Lett. A 142 (1989) 499.

[3] P.A. Hatherly, L.J. Frasinski, K. Codling, A.J. Langley, W. Shaikh, J. Phys. B: Atom. Mol. Phys. 23 (1990) L291.
[4] K. Codling, C. Cornaggia, L.J. Frasinski, P.A. Hatherly, J. Morellec, D. Normand, J. Phys. B: Atom. Mol. Phys. 23 (1991) L593.
[5] L.J. Frasinski, M. Stankiewicz, P.A. Hatherly, G.M. Cross, K. Codling, A.J. Langley, W. Shaikh, Phys. Rev. A 46 (1992) R6789.
[6] K. Codling, L.J. Frasinski, J. Phys. B: Atom. Mol. Phys. 26 (1993) 783.
[7] M. Stankiewicz, L.J. Frasinski, G.M. Cross, P.A. Hatherly, J. Phys. B: Atom. Mol. Phys. 26 (1993) 2619.
[8] K. Codling, L.J. Frasinski, Contemporary Phys. 35 (1994) 243.
[9] P.A. Hatherly, M. Stankiewicz, K. Codling, L.J. Frasinski, G.M. Cross, J. Phys. B: Atom. Mol. Phys. 27 (1994) 2993.
[10] L.J. Frasinski, P.A. Hatherly, K. Codling, M. Larsson, A. Persson, C.G. Wahlström, J. Phys. B: Atom. Mol. Phys. 27 (1994) L109.
[11] D.A. Card, D.E. Folmer, S. Sato, S.A. Buzza, A.W. Castleman Jr., J. Phys. Chem. A 101 (1997) 3417.
[12] D.A. Card, D.E. Folmer, S. Kooi, S. Sato, S.A. Buzza, A.W. Castleman Jr., Eur. J. Phys. D 9 (1999) 195.
[13] J. Purnell, E.M. Snyder, S. Wei, A.W. Castleman Jr., Chem. Phys. Lett. 229 (1994) 333.
[14] D.A. Card, D.E. Folmer, E.S. Wisniewski, A.W. Castleman Jr., J. Chem. Phys. 116 (2002) 3554.
[15] H. Budzikiewicz, C. Djerassi, D.H. Williams, Interpretation of Mass Spectra of Organic Compounds, Holden-Day, Inc., San Francisco, 1964.
[16] Q.N. Porter, Mass Spectrometry of Heterocyclic Compounds, 2nd ed., Wiley, New York, 1985.
[17] H. Ichikawa, M. Ogata, JACS 95 (1973) 806.
[18] I. Tokue, M. Ikarashi, Bull. Chem. Soc. Jpn. 54 (1981) 2565.
[19] J.H.D. Eland, J. Berkowitz, H. Schulte, R. Frey, Int. J. Mass Spectrom. Ion Phys. 28 (1978) 297.
[20] C. Kosmidis, P. Tzallas, K.W.D. Ledingham, T. McCanny, R.P. Singhal, P.F. Taday, A.J. Langley, J. Phys. Chem. A 103 (1999) 6950.
[21] J. Purnell, S. Wei, S.A. Buzza, A.W. Castleman Jr., J. Phys. Chem. 97 (1993) 12530.
[22] W.C. Wiley, I.H. McLaren, Rev. Sci. Instrum. 26 (1956) 1150.
[23] B.A. Mamyrin, V.I. Karataev, D.V. Shmikk, V.A. Zagulin, Sov. Phys. JETP 37 (1973) 45.
[24] J.W. Goodman, Statistical Optics, Wiley, New York, 1985.
[25] I. Noda, Appl. Spectrom. 47 (1993) 1329.
[26] S.M. Hurley, A.W. Castleman Jr., Science 292 (2001) 648.
[27] R.J. Levis, et al., Science 292 (2001) 709.
[28] M. Shapiro, P. Brumer, Advances in Atomic, Molecular and Optical Physics, in: B. Bederson, H. Walther (Eds.), vol. 42, Academic Press, San Diego, CA, 2000, p. 287.
[29] R.J. Gordon, et al., Acc. Chem. Res. 32 (1999) 1007.